Deep Learning-Based Method for Detecting Parkinson using 1D Convolutional Neural Networks and Improved Jellyfish Algorithms

Original Scientific Paper

Arogia Victor Paul M*
Department of Computer Science and Engineering,
B.S. Abdur Rahman Crescent Institute of Science and Technology, Chennai, India
victorpaul_cse@crescent.education

Sharmila Sankar
Department of Computer Science and Engineering,
B.S. Abdur Rahman Crescent Institute of Science and Technology, Chennai, India
sharmilasankar@crescent.education

*Corresponding author

Abstract *– Parkinson's disease (PD) is a common disease that predominantly impacts the motor scheme of the neural central scheme. While the primary symptoms of Parkinson's disease overlap with those of other conditions, an accurate diagnosis typically relies on extensive neurological, psychiatric, and physical examinations. Consequently, numerous autonomous diagnostic assistance systems, based on machine learning (ML) methodologies, have emerged to assist in evaluating patients with PD. This work proposes a novel deep learning-based classification of Parkinson's disease (PD) using voice recordings of people into normal, idiopathic Parkinson, and familial Parkinson. The improved jellyfish algorithm (IJFA) is utilized for hyper-parameter selection (HPS) of a 1D convolutional neural network (1D-CNN). The proposed technique makes use of the significant elements of 1D-CNN and filter-based feature selection models. Because of their strong performance in dealing with noisy data, the filter-based algorithms Relief, mRMR, and Fisher Score were chosen as the top choices. Using just 62 characteristics, the combination of deep relief features and deep learning was able to discriminate between people. The competence of the proposed 1D-CNN with IJFA method was determined through specific network metrics. The proposed 1D-CNN with IJFA method attains a total accuracy of 98.6%, which is comparatively better than the existing techniques. The proposed model produced around 9.5% improvements in accuracy, respectively, when compared to the data obtained without dimensionality reduction.*

Keywords: *Parkinson Disease Classification, Convolutional Neural Network, Improved jellyfish algorithm, Filter-based feature selection model*

Received: January 10, 2024; Received in revised form: March 1, 2024; Accepted: April 8, 2024

1. INTRODUCTION

Parkinson Disease (PD) is a condition that touches the motor scheme of the dominant nervous organization of the human body. Motor symptoms and non-motor symptoms are the two categories that may be used to describe the symptoms of PD [1]. The motor symptoms involve trembling and a lack of energy in the hands and legs, constipation, difficulty doing daily tasks, and a shuffled gait when walking [2]. Parkinson's disease non-motor symptoms include a variety of problems, including weariness, constipation, difficulty speaking, memory loss, and exhaustion [3]. Studies suggest that voice problems arise in about 90 percent of PD cases [4]. The Procedure of Diagnosing (PD) using just certain qualitative criteria may make the process more difficult since other illnesses might also present with similar symptoms [5].

In recent years, a surge in Parkinson's disease research has leveraged machine learning (ML) for diagnosis [6]. Studies have utilized various data, including walking tracks, speech recordings, and brain electrical event recordings (EEG) [7]. Notably, speech-based diagnostic methods have shown promise, as speech difficulties often manifest early in PD [8]. These algorithms effectively distinguish between individuals with PD and healthy subjects using distinctive features extracted from raw speech data [9]. PD diagnostic systems employ diverse speech signal processing algorithms to extract clinical-

ly relevant vocal characteristics from voice recordings [10]. Essential features extracted from real-world datasets are input into machine learning models for PD diagnosis [11]. The performance of these models depends on the relevance of features utilized during training [12]. To address high dimensionality and sparse data issues, reducing dimensionality is crucial in PD research. This process emphasizes relevant characteristics, enhancing the success of machine learning models for diagnosis [13, 14]. The contribution of this paper is,

- In this work, proposed a novel deep learning-based classification of Parkinson's disease using voice recordings of people into normal, idiopathic Parkinson, and familial Parkinson.
- Initially, the CNN network is used as a feature extractor to extract the voice recordings.
- Then, the Improved Jellyfish Search Algorithm (IJFA) to select the features before the final layers is utilized for hyper-parameter selection (HPS) of 1D-convolutional neural network (1D-CNN).
- Finally, a 1D-CNN classifier was trained using the generated deep feature representations.
- The performance of the Proposed 1D-CNN with IJFA method was measured by parameters such as Specificity, Accuracy, F1 score, Precision, and Sensitivity.

In Section 2, we provide the work that is relevant to this study, and in Section 3, we provide an explanation of the suggested model. Sections 4 and 5 each provide a conclusion that summarises the findings of the validation study.

2. RELATED WORKS

Recent research has presented various deep learning-based methods for detecting Parkinson's disease.

In 2022, Sahu et al. [15] suggested an early Parkinson disease diagnosis method based on hybrid deep learning. The combination of two deep learning techniques, such as regression analysis (RA) and artificial neural networks (ANN), for efficient probability-based illness diagnosis. The accuracy of the suggested method is 93.46%.

In 2022, Vyas et al. [16] developed a method for deep learning (DL) that uses convolutional neural networks (CNNs) in two and three dimensions. The 2D model attained an accuracy of 72.22% with 0.50 area under the curve (AUC), whereas the 3D model features from the data were able to categorize the test data with an accuracy of 88.9% with 0.86 AUC.

In 2022, Hosny et al. [17] developed a brand-new deep learning model to identify subthalamic nuclei (STN) in signals from local field potentials (LFPs). The k-Nearest Neighbor (KNN) classifier receives the characteristics as input. According to the findings, KNN achieved an accuracy rate of 87.27% on average.

In 2022, Rajanbabu et al. [18] developed transfer learning-based deep learning architectures for effective PD diagnosis using MRI data. Based on the maximum chance of all the models chosen for PD classification, an ensemble model is suggested. The method primarily concentrates on providing an accurate PD diagnosis.

In 2022, Moradi et al. [19] offered a microarray dataset (GSE22491) that was given by GEO. The Limma package, which is part of the R program, was used to find DEGs and analyze and assess gene expression. Support vector machines (SVM) results show that using three genes together can lead to an 88% prediction accuracy.

In 2022, AlMahadin et al. [20] proposed a series of resampling methods to enhance the classification of tremor severity in Parkinson's disease. The suggested method combines three types of resampling and signal processing techniques: hybrid, under, and over-sampling. ANN-MLP, as suggested, has an overall accuracy of 93.81%.

In 2024, Canturk et al. [21] suggested utilizing voice signals and artificial intelligence to diagnose Parkinson's disease. AlexNet, GoogleNet, ResNet50, and the majority of voting-based hybrid systems are among the first classifiers used. The deep feature fusion method produced an accuracy of 0.95%.

In 2024, Aldhyani et al. [22] suggested that the public dataset PD Spiral Drawings be utilized for PD research and diagnosis. The suggested technique made use of a common dataset made up of 204 spiral and wave drawings made by people with Parkinson's disease. With 94% accuracy, pictures were used to train the DenseNet201 classifier.

The analysis highlighted earlier emphasizes the constraints of current research procedures and models. To overcome these limitations, this paper Improved jellyfish algorithm (IJFA) is utilised for hyper-parameter selection (HPS) of 1D-convolutional neural network (1D-CNN).

3. PROPOSED METHODOLOGY

3.1. DATASET DESCRIPTION

In this proposed method, the Parkinson's disease dataset can be used. In this dataset, there are 62 voice recordings of people. Also, this dataset consists of three class: 50% samples belonging to healthy and 50% samples belonging to patients. The data in PD dataset take from 62 patients with Parkinson Disease (30 men and 32 women) with ages ranging from 33 to 87. The PD dataset with the of 50-50% training and testing partition.

3.2. FEATURES SELECTION

In medical applications, feature selection has been the subject of several research, all of which have shown that it is both adequate and successful. Because it is a

pre-processing method, it is able to single out the most important aspect of the issue. Maximum relevance redundant features as feasible (minimum redundancy). Maximum relevance seeks to identify the characteristics that it also seeks to give the feature subset comprising fewer and minimal redundant features as feasible.

According to the mRMR, the optimization condition ought to be expressed as follows:

$$x_j \in X - S_{k-1} Max\ [I(x_j, c) - \frac{1}{k-1}\sum_{x_i \in S_{k-1}}^{n} I(x_j, x_i)] \quad (1)$$

When c is the target class, x_i is the ith feature, and X is the entire set of features. The mutual information between class c and feature x_j is represented by x_i.

The mRMR method improves classification accuracy while simultaneously reducing the number of variables used. This is accomplished by minimising the selection of duplicate features. Table 1 shows the different aspects of the human voice.

Table 1. Different aspects of human voice

Description	Voice measure
11-point Amplitude Perturbation Quotient	MDVP: APQ
Absolute jitter in microseconds	MDVP: Jitter (Abs)
Average vocal fundamental incidence	MDVP: F0 (Hz)
Maximum vocal fundamental incidence	MDVP: Fhi (Hz)
Relative Amplitude Perturbation	MDVP: RAP
Five-point Period Perturbation Quotient	MDVP: PPQ
Average absolute difference of differences among cycles, divided by the average period	Jitter: DDP
Shimmer Local amplitude perturbation	MDVP: Shimmer
Local amplitude perturbation	MDVP: Shimmer (db)
Average absolute difference among the amplitudes of consecutive aeras	Shimmer: DDA
Noise-to-Harmonics Relation	NHR
Harmonics-to-Noise Relation	HNR
Recurrence Period Density Entropy	RPDE
Correlation Dimension	D2
Fundamental frequency difference	Spread1
Fundamental frequency difference	Spread2
Pitch retro entropy	PPE

$$f(K) = \frac{\sum_{j=1}^{C} n_j \left(\mu_j^l - \mu^l\right)^2}{\sum_{j=1}^{C} n_j \left(\sigma_j^l\right)2} \quad (2)$$

The number of occurrences of a feature is denoted by its mean, which is denoted by the symbol l, whereas the number of occurrences of a class is denoted by the symbol n j. During the process of feature selection using Fisher Score, all of the features are sorted in decreasing order beginning with the high scores are selected.

3.2.2. Relief

The significance of the features is computed via relief selection, which does this by illuminating the relationships that exist between the features and the class labels. The iterative process that was used in order to indicate the feature relevances may be seen in the equation (3).

$$W_i = W_{i-1} - (x_i - NearHit_i)^2 + (x_i - NearMiss_i)^2 \quad (3)$$

In the 'n' dimensions and records of n different characteristics. While the closest samples of the same class and those of different classes are denoted by the terms "NearHit" and "NearMiss," respectively.

3.3. 1D-CNN FOR CLASSIFICATION

In convolution neural network (CNN) models are used rather often for the purpose of image identification in two dimensions. On the other hand, the use of CNN models should not be limited to either two-dimensional or tasks in order to be utilised. It should come as no surprise that the 1D-CNN model has the same qualities as previous CNN models. A one-dimensional input signal, which will be indicated by S, and a kernel variable, which will be denoted by W will be used in the following description of the convolution procedure.

$$(S * W)_n = \sum_{i=1}^{|w|} W(i) S(i + n - 1) \quad (4)$$

A feature map is the term used to refer to the final product of the convolution process. Let the limited matrix of the input matrix to the weight matrix be denoted by the notation $S_{|W(i,j)}n$. $S_{|W(i,j)}n$ is a representation of the elements of S from n up to the dimension of $W(i,j)$. As a result, the output matrix is capable of being characterised by a generic formula, which may be found in Equation (5):

$$O_n^l = \left(S_{|W(i,j)} * W(i,j)\right)_n \quad (5)$$

The final part of the CNN model, which usually consists of a neural network layer, handles the classification task. This layer is in charge of the final level and is referred to as a completely connected layer. The input consists of the pre-processed signal segments, each of which contains 50% samples. In the first layer of the model, the signals are convoluted using 64 x 5 filters and three stride ratios in order to build feature maps with sizes ranging from 64 x 999 to 64 x 999. The second layer of the model is also a convolution layer has 128 filters by 5 rows. This layer produces brand new feature maps by using the results of the previous layer.

The Max Pool layer combines the two output vectors' maximum values in two-unit areas into a single value. This value is the result of the condensing process. These steps are repeated in a similar way in each of the model's subsequent layers, but each time, a range of distinct filter sizes are used. Dropout layers are built into the model to reduce the issue of overfitting. The dimensions determined in the flattened layer must be changed to fit the thick layers. The final layer, the softmax layer, is where the input signals are mapped onto the output signals. Therefore, the sum of classes (nb class) and the sum of units (nb unit) in this layer are equal to one another. In CNN network at the end of the last convolution, they apply the Jellyfish Search

Algorithm to select the features before the final layers. Table 2 contains comprehensive parameter representations of all of the model's layers. The Proposed 1D-CNN model is shown in Fig. 1.

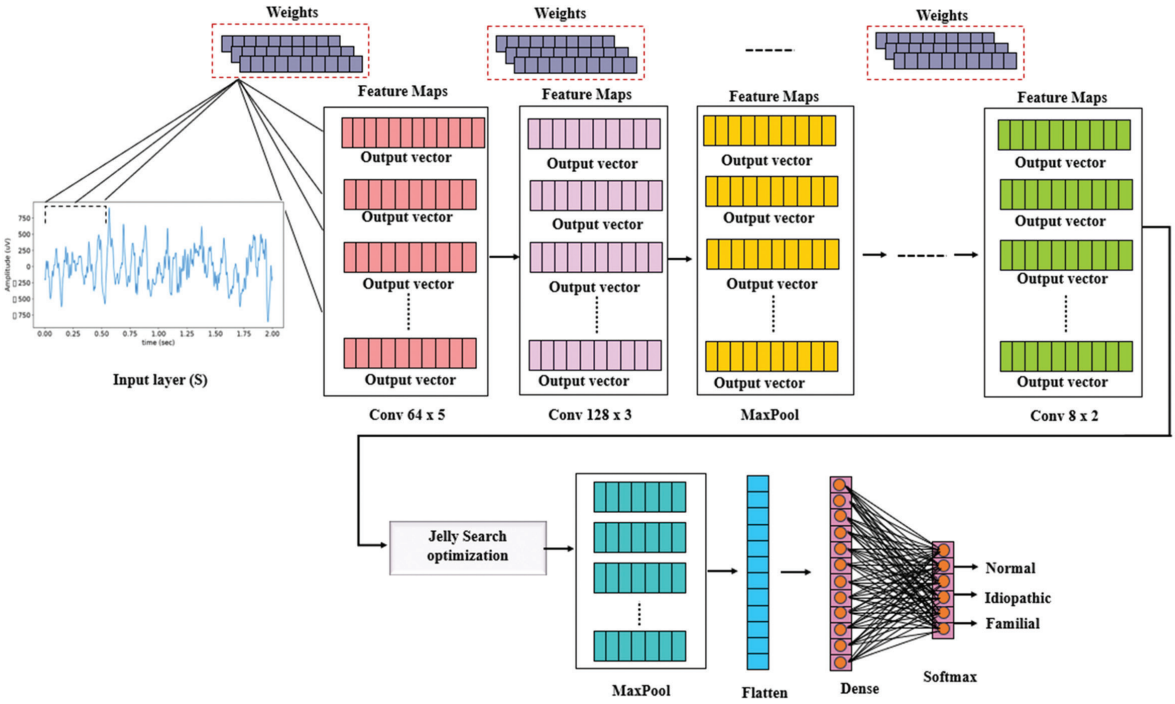

Fig. 1. The Architecture of the proposed 1D-CNN model

Table 2. Particulars of layers and strictures in the projected 1D-CNN perfect

Layer Name	Sum of Filter× Kernel Size	Sum of Trainable Parameters	Layer Parameters	Region/Unit Size	Output Scope
1D Conv	64 × 5	384	ReLU, S = 3	-	64 × 999
1D Conv	128 × 5	24,704	ReLU, Stride = 1	-	128 × 997
MaxPool	-	0	S = 2	2	128 × 489
Dropout	-	0	Rate = 0.2	-	128 × 498
1D Conv	128 × 13	213,120	ReLU, S = 1	-	128 × 346
1D Conv	256 × 7	229,632	ReLU, S = 1	-	256 × 480
MaxPool	-	0	Stride = 2	2	256 × 240
1D Conv	256 × 7	262,272	ReLU, S = 1	-	128 × 322
1D Conv	64 × 4	32,832	ReLU, S = 1	-	64 × 230
MaxPool	-	0	Stride = 2	2	64 × 54
1D Conv	8 × 5	2568	ReLU, S = 1	-	8 × 50
1D Conv	8 × 2	136	ReLU, S = 1	-	8 × 49
MaxPool	-	0	Stride = 2	2	8 × 42
Flatten	-	0	-	-	1 × 192
Dense	-	12,352	ReLU, Drop = 0.2	64	1 × 64
Dense	-	195	Softmax	nb_class	1 × nb_class

3.3.1. Jellyfish Search Algorithm

The search-feeding behaviour and drive designs of jellyfish in the water served as an inspiration for the development of the algorithm. The following is a rundown of the three rules that are a part of the JS algorithm:

Rule 1: Jellyfish are able to move in two different ways: one is to follow the currents of the ocean, and the other is to move about within their own population. The transition between these two different forms of drive is accomplished via a time- process.

Rule 2: Jellyfish habit, and when they are looking for food in the water, they are drawn to areas that have a greater concentration of food for them to consume.

Rule 3: stipulates that the quantity of food that jellyfish look for is reliant on the geographical location of the food as well as the goal purpose of the reaction. This model includes mechanisms for group movement, movement in response to time, and movement of jellyfish that follow the movement of ocean currents.

(1) Following ocean current movement

The term "trend" is used to describe the direction in which the current is moving.

$$trend \rightarrow = \frac{1}{n_{pop}} \sum_{i=1}^{n_{pop}} trend_i \rightarrow \quad (6)$$

where, n_{pop} is the present optimum position, and the equation that specifies its relationship is as follows:

$$trend_i \rightarrow = X^* - e_c X_i \quad (7)$$

where X^* represents the equation is derived by iterating over the previous equation until the desired result is achieved:

$$trend \rightarrow = \frac{1}{n_{pop}} \sum_{i=1}^{n_{pop}} (X^* - e_c X_i) = X^* - e_c \frac{1}{n_{pop}} \sum_{i=1}^{n_{pop}} X_i = X^* - e_c \mu \quad (8)$$

where *m* is the average location of all of the jellyfish. DF is represented as shadows:

$$DF = e_c \mu \quad (9)$$

The following is what you get when you plug Equation (9) into the equation that describes the ideal position:

$$trend \rightarrow = X^* - DF \quad (10)$$

The distribution of Jellyfish in the ocean is shown is Fig. 2. Where σ is the standard deviation of the normal distribution, and β signifies the distribution coefficient, which set to 3 in the algorithm. The range of $\pm\beta\sigma$ around the mean position μ contains the probability of all jellyfish positions.

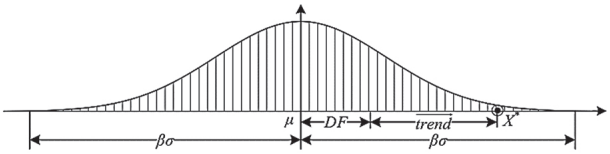

Fig. 2. Normal distribution of jellyfish in the ocean

A relative investigation demonstration that e_c can be uttered as shadows:

$$e_c = \beta * rand(0,1) \quad (11)$$

Following is the equation that was acquired in order to derive the equation

$$X_i(t+1) = X_i(t) + rand(0,1) * trend \rightarrow = X_i(t) + rand(0,1) * (X^* - \beta * rand(0,1) * \mu \quad (12)$$

where X i (t) represents the location of the Jellyfish at the instant in time when its position is being updated, and X i (t+1) represents the position of the jellyfish

(2) Movements made in groups

The jellyfish moves in a circle around its current position to indicate class A movement, and the following equation is used to update the jellyfish's position

$$X_i(t+1) = X_i(t) + \gamma * rand(0,1) * (U_b - L_b) \quad (13)$$

where *g* is the jellyfish's mobility coefficient, *Lb* is the lower bound, and *Ub* is the upper limit of the search space.

The following formula can be used to update the location of jellyfish participating in Class B drive: jellyfish that gather with the intention of consuming food when there is more food around:

$$X_i(t+1) = X_i(t) + step \rightarrow \quad (14)$$

where, *step*→ signifies the step length of jellyfish

defines *step*→ and is uttered as follows:

$$step \rightarrow = rand(0,1) * D \rightarrow \quad (15)$$

where, *D*→ shows the direction in which the jellyfish are swimming i. The following is an expression of the formula that may be used to determine the direction of motion:

$$D \rightarrow = \begin{cases} X_j(t) - X_i(t), iff\left(X_i(t)\right) \geq f\left(X_j(t)\right) X_i(t) - \\ X_j(t), iff(X_j(t)) \geq f(X_i(t)) \end{cases} \quad (16)$$

where X_i (*t*) signifies the current location of jellyfish I, X_j (*t*) represents tof jellyfish *j*, function *f* represents the objective function with regard to *X*, and *X* signifies the collection of all jellyfish.

(3) A strategy for managing time

A temporal control system had to be conceived of, developed, and put into operation in order to successfully reproduce and materialise the switching that jellyfish are capable of doing between their three different modes of motion. The mechanism in question was described as a time control function denoted by the letter *c*. (*t*).

This is an expression of the formula that defines the variable *c* as follows: (*t*):

$$c(t) = \left|\left(1 - \frac{t}{T}\right) * (2 * rand(0,1) - 1)\right| \quad (17$$

where *t* is the current number of iterations, *T* is the number of iterations, and *c*(*t*) is a value that is randomly generated between 0 and 1 for each iteration. It was found that the range of values that controlled the jellyfish's movement in reaction to ocean currents was *c*(*t*) 0.5.

3.3.2. Improved Jellyfish Search Procedure

The (IJS) algorithm is presented in this section, and a thorough explanation of it can be found as follows:

(1) Development of a better technique for the initialization of population placement

Both the Sobol arrangement and the chaotic mapping starting strategy were used in order to create fifty percent of the total population. Under the illness that the search range limitation is satisfied, the Sobol sequence has the potential to create the beginning location of the jellyfish population in a more consistent manner. The functional representation of tent mapping may be described as follows:

$$x_{t+1} = \begin{cases} \frac{x_t}{\alpha} x_t \in [0, \alpha](1 - x_t)/(1 - \alpha)\ x_t \in (\alpha, 1) \end{cases} \quad (18)$$

where x t is the created chaotic sequence, t2 is a series of numbers from 1 to n, n is the sum that has to be initialised, and an is an adjustment parameter with a value of 0.5.

(2) A sinusoidal component in the dynamic adaptation

A sinusoidal was included into the artificial jellyfish search algorithm in order to enhance its capacity for doing local searches. The expression of this factor may be expressed as follows:

$$S = 1 + sin\ sin\frac{\pi(2T+t)}{2T} \quad (19)$$

where S stands for the sinusoidal lively adaptation factor, T for the maximum iterations, and t for the iterations that are currently being performed.

(3) The functioning of the population difference

As the following explains, the addition of the random variation operation to the artificial jellyfish search method aimed to enhance the capacity to do worldwide searches and broaden the population's diversity:

Operation 1: After the jellyfish had finished migrating in accordance with the position update formula and had computed their respective fitness values, a particular jellyfish from the existing population was selected and given the name X_k. This particular jellyfish was picked at random. Next, three different jellyfish individuals were selected at random, and their relative fitness values were ranked from best to worst in order to determine X_a, X_b, and X_c. These individuals' fitness values are represented by the letters fa, fb, and fc, respectively. Finally, the following is an expression of the formula that may be used to calculate the new location of X_k:

$$X_k = X_a + \delta(X_b - X_c) \quad (20)$$

where d represents the variational operator, and the formula for it may be written as follows:

$$\delta = \delta_l + (\delta_u - \delta l) * \frac{f_b - f_a}{f_c - f_a} \quad (21)$$

where δ_u and dl represent the top and lower boundaries of variability, with 0.9 and 0.1 being the values used, respectively.

4. EXPERIMENTAL RESULTS AND DISCUSSION

The overall performance of the Proposed 1D-CNN with IJFA method was evaluated built on the specific parameters viz., Accuracy, Precision, F1 score, Sensitivity, and Specificity.

$$\text{Sensitivity} = \frac{TP}{TP+FP} \quad (22)$$

$$\text{Specificity} = \frac{TN}{TN+FP} \quad (23)$$

$$Accuracy = \frac{\#Number\ of\ correct\ predictions}{\#Total\ number\ of\ predictions} \quad (24)$$

$$\text{Precision} = \frac{TP}{TP+FP} \quad (25)$$

$$F1Score = \frac{2TP}{2TP+FP+FN} \quad (26)$$

False positives and true negatives of the MRI images are designated as TP and FP, respectively, whereas false positives and true negatives are designated as TN and FN, respectively. Table 2 shows the parameters for PD classes that are used to determine the proposed model's performance analysis.

Table 3. The overall Performance analysis of the Proposed model

Class	Accuracy	Precision	Sensitivity	F1-score	Specificity
Normal	97.54	96.32	94.08	93.69	92.58
Idiopathic	95.09	94.28	93.75	92.07	91.19
Familial	96.46	95.32	94.66	93.97	93.33

Table 1 illustrations the classification of various classes of Parkinson disease with specific metrics. The average Specificity, F1 score, Accuracy, Sensitivity, and Precision of the proposed 1D-CNN with IJFA method with the specific metrics. The proposed 1D-CNN with IJFA method has an average precision, sensitivity, F1score, and specificity of 95.3%, 94.16%, 93.24%, and 92.36%, respectively. Fig. 3 shown the performance parameters for three classes.

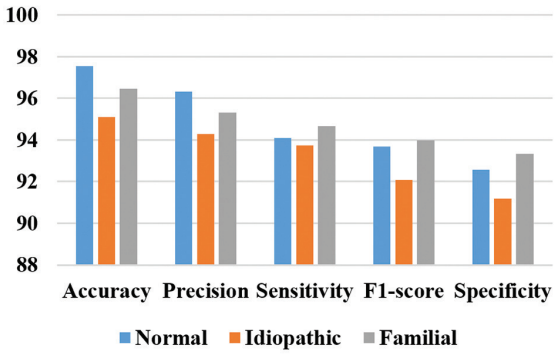

Fig. 3. The overall performance analysis of the proposed model

4.1. FEATURES SELECTION RESULTS

Maximum relevance minimal redundancy: selected the traits that were the most significant to us by using the mRMR, which stands for minimum redundancy (22 features). The PPE is the single most important variable in predicting the result. There is a noticeable difference between the first feature and the rest of the features combined because the first feature has a significantly lower score. The algorithm is positive; it has selected the most significant predictor because of the notable drop in the value of the relevant variable. Other research has demonstrated that, in contrast to earlier evaluations, PPE is resistant to the effects of noisy auditory environments and is also sensitive to changes in PD speech. Subsequently, the entropy is computed using the probability distribution of the semitone variations to define the PPE measure. Converting a speech pitch pattern into a logarithmic semitone measure is the first step in creating the probability distribution. Fig. 4 illustrates a sampling of the findings from this criterion selection. Fig. 5 displays the 22 characteristics in the feature ranking discovered by Relief.

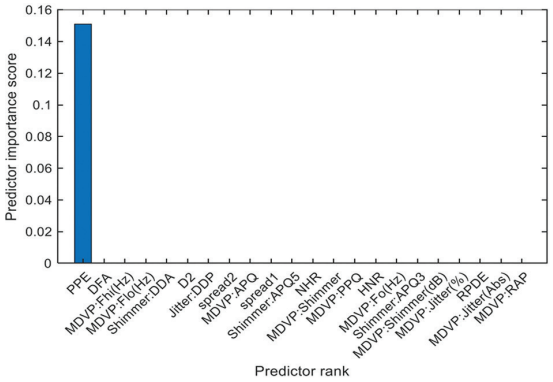

Fig. 4. Samples of the Feature findings

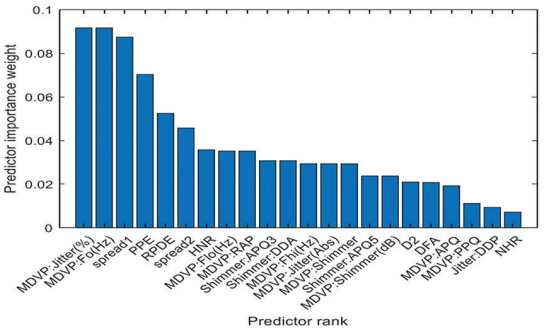

Fig. 5. The 22 characteristics of feature Ranking for Relief

The degree of relevance weights of all characteristics is figured out with the help of the bar plot. The Performance Analysis for Classifier is shown in Table 3. Fig. 6 provides the graphical analysis of proposed model with existing techniques.

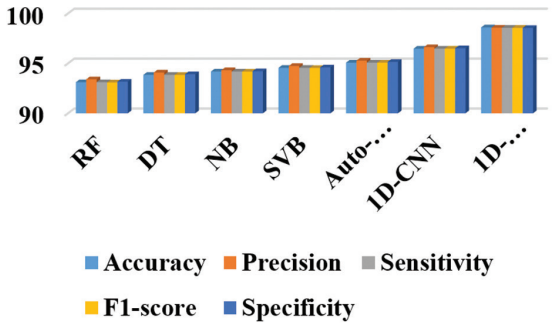

Fig. 6. Comparative Analysis of Proposed Model

Table. 4. Comparison of the proposed and the existing models

Authors	Methods	Accuracy
Sahu [15]	ANN-RA	93.46%
Vyas [16]	2D-CNN	88.9%
Hosny [17]	CNN-KNN	87.27%
AlMahadin [20]	ANN-MLP	93.81%
Proposed	1D-CNN with IJFA	98.6%

From Table 4, the comparison of several deep learning techniques based on their accuracy in the PD signals.

The Proposed 1D-CNN with IJFA method advances the overall accuracy by 5.21%, 9.83%, 11.4%, and 4.85% better than ANN-RA [13], 2D-CNN [15], CNN-KNN [16], and ANN-MLP [19] respectively. It is obvious from Table 4 that our innovative network outperforms the current methods. As a result, the proposed 1D-CNN with IJFA method fallouts may be used to accurately classify the PD disease.

Table 5. Performance Analysis for Classifier

Model	Accuracy	Precision	Sensitivity	F1-score	Specificity
RF	93.11	93.4	93.11	93.09	93.16
DT	93.85	94.08	93.85	93.84	93.91
NB	94.18	94.31	94.18	94.17	94.21
SVB	94.55	94.74	94.55	94.54	94.59
Auto-encoder	95.07	95.27	95.07	95.07	95.14
1D-CNN	96.47	96.62	96.47	96.47	96.51
1D-CNN with IJFA	98.6	98.57	98.56	98.56	98.54

5. CONCLUSION

This paper presents a novel deep learning-based classification of Parkinson's disease using voice recordings of people into normal, idiopathic Parkinson, and familial Parkinson. The improved jellyfish algorithm (IJFA) is utilized for hyper-parameter selection (HPS) of a 1D convolutional neural network (1D-CNN). To differentiate Parkinson's patients from healthy individuals at an early stage, the 1D-CNN method, coupled with IJFA approaches, was employed. The proposed technique takes use of the significant elements of 1D-CNN and filter-based feature selection models. In comparison between the other techniques the proposed 1D-CNN with IJFA methods with the accuracy of 98.6%. In the future, deep feature representations will be extracted from various kinds of data sources collected from wearable sensors, and then these data sources will be combined with various multi-modal techniques.

6. REFERENCES:

[1] N. Bhore, E. C. Bogacki, B. O'Callaghan, P.-H. Favreau, P. A. Lewis, S. Herbst, "Common genetic risk for Parkinson's disease and dysfunction of the endo-lysosomal system", Philosophical Transactions of the Royal Society B, Vol. 379, No. 1899, 2024, p. 20220517.

[2] S. Parveen, J. Moore, "Current Perceptions and Unmet Needs of People with Parkinson Disease and their Families", Clinical Archives of Communication Disorders, Vol. 8, No. 2, 2023, pp. 57-69.

[3] P. Ananthavarathan, B. Patel, S. Peeros, R. Obrocki, N. Malek, "Neurological update: non-motor symptoms in atypical parkinsonian syndromes", Journal of Neurology, Vol. 270, 2023, pp. 4558-4578.

[4] T. Romero Arias, I. R. Cortés, A. P. del Olmo, "Biomechanical parameters of voice in Parkinson's disease patients", Folia Phoniatrica et Logopaedica, Vol. 76, No. 1, 2024, pp. 91-101.

[5] M. T. García-Ordás, J. A. Benítez-Andrades, J. Aveleira-Mata, J. M. Alija-Pérez, C. Benavides, Determining the severity of Parkinson's disease in patients using a multi task neural network. Multimedia Tools and Applications, Vol. 83, No. 2, 2024, pp. 6077-6092.

[6] A. H. Al-nefaie, T. H. Aldhyani, D. Koundal, "Developing System-based Voice Features for Detecting Parkinson's Disease Using Machine Learning Algorithms", Journal of Disability Research, Vol. 3, No. 1, 2024, p. 20240001.

[7] S. Zhao, G. Dai, J. Li, X. Zhu, X. Huang, Y. Li, M. Tan, L. Wang, P. Fang, X. Chen, N. Yan, "An interpretable model based on graph learning for diagnosis of Parkinson's disease with voice-related EEG", NPJ Digital Medicine, Vol. 7, No. 1, 2024, p. 3.

[8] L. Cardenas, K. Parajes, M. Zhu, S. Zhai, "Auto-Health: Advanced LLM-Empowered Wearable Personalized Medical Butler for Parkinson's Disease Management", Proceedings of the IEEE 14th Annual Computing and Communication Workshop and Conference, Las Vegas, NV, USA, 8-10 January 2024, pp. 375-379.

[9] L. Ali, A. Javeed, A. Noor, H. T. Rauf, S. Kadry, A. H. Gandomi, "Parkinson's disease detection based on features refinement through L1 regularized SVM and deep neural network", Scientific Reports, Vol. 14, No. 1, 2024, p. 1333.

[10] T. D. Pham, S. B. Holmes, L. Zou, M. Patel, P. Coulthard, "Diagnosis of pathological speech with streamlined features for long short-term memory learning", Computers in Biology and Medicine, Vol. 170, 2024, p. 107976.

[11] J. Varghese, A. Brenner, M. Fujarski, C. M. van Alen, L. Plagwitz, T. Warnecke, "Machine Learning in the Parkinson's disease smartwatch (PADS) dataset", NPJ Parkinson's Disease, Vol. 10, No. 1, 2024, p. 9.

[12] L. Ali, C. Chakraborty, Z. He, W. Cao, Y. Imrana, J. J. Rodrigues, "A novel sample and feature dependent ensemble approach for Parkinson's disease detection", Neural Computing and Applications, Vol. 35, No. 22, 2023, pp. 15997-16010.

[13] R. Kapila, S. Saleti, "Optimizing Predictive Models for Parkinson's Disease Diagnosis", Intelligent Technologies and Parkinson's Disease: Prediction and Diagnosis, IGI Global, 2024, pp. 255-275.

[14] M. Shivakoti, S. C. Medaramatla, D. Godavarthi, N. Shivakoti, "Prognoza: Parkinson's Disease Prediction Using Classification Algorithms", EAI Endorsed Transactions on Pervasive Health and Technology, Vol. 9, 2023.

[15] L. Sahu, R. Sharma, I. Sahu, M. Das, B. Sahu, R. Kumar, "Efficient detection of Parkinson's disease using deep learning techniques over medical data", Expert Systems, Vol. 39, No. 3, 2022, p. e12787.

[16] T. Vyas, R. Yadav, C. Solanki, R. Darji, S. Desai, S. Tanwar, "Deep learning-based scheme to diagnose Parkinson's disease", Expert Systems, Vol. 39, No. 3, 2022, p. e12739.

[17] M. Hosny, M. Zhu, W. Gao, Y. Fu, "A novel deep learning model for STN localization from LFPs in Parkinson's disease", Biomedical Signal Processing and Control, Vol. 77, 2022, p. 103830.

[18] K. Rajanbabu, I. K. Veetil, V. Sowmya, E. A. Gopalakrishnan, K. P. Soman, "Ensemble of Deep Transfer Learning Models for Parkinson's Disease Classification", Soft Computing and Signal Processing, Vol. 1340, Springer, 2022, pp. 135-143.

[19] S. Moradi, L. Tapak, S. Afshar, "Identification of Novel Noninvasive Diagnostics Biomarkers in the Parkinson's Diseases and Improving the Disease Classification Using Support Vector Machine", BioMed Research International, Vol. 2022, 2022.

[20] G. AlMahadin, A. Lotfi, M. M. Carthy, P. Breedon, "Enhanced Parkinson's disease tremor severity classification by combining signal processing with resampling techniques", SN Computer Science, Vol. 3, No 1, 2022, pp. 1-21.

[21] İ. Canturk, O. Günay, "Investigation of Scalograms with a Deep Feature Fusion Approach for Detection of Parkinson's Disease", Cognitive Computation, 2024, pp. 1-12.

[22] T. H. Aldhyani, A. H. Al-Nefaie, D. Koundal, "Modeling and diagnosis Parkinson disease by using hand drawing: deep learning model", AIMS Mathematics, Vol. 9, No. 3, 2024, pp. 6850-6877.